Hydromagnetic combined heat and mass transfer by natural convection from a permeable surface embedded in a fluid-saturated porous medium

Received September 1999
Revised February 2000
Accepted April 2000

Ali J. Chamkha and Abdul-Rahim A. Khaled
Department of Mechanical and Industrial Engineering, Kuwait University, Safat, Kuwait

Keywords *Natural convection, Heat transfer, Hydromagnetics, Coupled phenomena*

Abstract *The problem of coupled heat and mass transfer by natural convection from a vertical, semi-infinite flat plate embedded in a porous medium in the presence of an external magnetic field and internal heat generation or absorption effects is formulated. The plate surface is maintained at either constant temperature or constant heat flux and is permeable to allow for possible fluid wall suction or blowing. The resulting governing equations are non-dimensionalized and transformed using a non-similarity transformation and then solved numerically by an implicit, iterative, finite-difference scheme. Comparisons with previously published work are performed and excellent agreement is obtained. Useful correlations containing the various physical parameters for both isothermal and isoflux wall conditions are reported. A parametric study of all involved parameters is conducted and a representative set of numerical results for the velocity, temperature and concentration profiles as well as the skin-friction parameter, Nusselt number, and the Sherwood number is illustrated graphically to show typical trends of the solutions.*

Nomenclature

A	= inverse Darcy number	F	= inertia coefficient of the porous medium
B	= inertia coefficient parameter		
B_o	= magnetic field strength	f	= dimensionless stream function
C	= concentration at any point in the field	g	= gravitational acceleration
		H	= magnetic dissipation parameter
C_o	= concentration at the wall for (UWT)	h	= local convective heat transfer coefficient
C_∞	= concentration at the free stream	$\overline{h}$	= average convective heat transfer coefficient
C_w	= concentration at the wall for (UHF)		
C_{wo}	= reference concentration for (UHF)	h_m	= local mass transfer coefficient
c	= dimensionless concentration at any point	$\overline{h}_m$	= average mass transfer coefficient
		K	= permeability of the porous medium
c_o	= dimensionless concentration at the wall for (UWT)	k_e	= effective thermal conductivity of the porous medium
c_p	= specific heat of the ambient fluid	L	= characteristic length of the plate
D	= mass diffusivity	Le	= Lewis number
Ec	= Eckert number	M	= square of the Hartmann number
e	= buoyancy ratio	Nu	= local Nusselt number

International Journal of Numerical Methods for Heat & Fluid Flow, Vol. 10 No. 5, 2000, pp. 455-476.

Nu_{AVG} = average Nusselt number
Pr = Prandtl number
Q = internal heat generation or absorption coefficient
Q_o = dimensionless heat transfer at the wall for (UHF)
q_o = heat flux at the wall for (UHF)
R = dimensionless temperature
R_o = dimensionless temperature at the wall for (UWT)
Sh_x = local Sherwood number
Sh_{AVG} = average Sherwood number
T = temperature at any point
T_o = wall temperature for (UWT)
U = tangential velocity
UHF = uniform wall heat flux
UWT = uniform wall temperature
u = dimensionless tangential velocity
V = normal velocity
V_o = dimensionless blowing or injection velocity
v_o = blowing or injection velocity
X = distance along the plate
x = dimensionless distance along the plate
Y = distance normal to the plate
y = dimensionless distance normal to the plate

Greek symbols

α_e = effective thermal diffusivity of the porous medium
β_c = concentration expansion coefficient
β_T = thermal expansion coefficient
ς = transformed concentration
η = coordinate transformation in terms of x and y
ε = porosity of the porous medium
ϕ = internal heat generation or absorption parameter
μ = dynamic viscosity
υ = kinematic viscosity
ψ = stream function
θ = transformed temperature
τ_w = wall shear stress
ρ = fluid density
σ = fluid electrical conductivity
ξ = coordinate transformation for x

Introduction

Coupled heat and mass transfer in fluid-saturated porous media finds applications in a variety of engineering processes such as in heat exchanger devices, insulation systems, petroleum reservoirs, magnetohydrodynamic (MHD) accelerators and generators, filtration, chemical catalytic reactors and processes, nuclear waste repositories and problems of soil contamination by crude oil as that occurred in the State of Kuwait during the Gulf War. In addition, coupled heat and mass transfer can interpret certain natural phenomena such as ocean currents driven by differential heating and act as freight trains for salt as mentioned by Bejan (1993), and the role of factory waste gas diffusion in a differential heating circulated air. There has been considerable work done on the study of flow and heat transfer in geometries with and without porous media (for instance, Vafai and Tien (1981) and Churchill and Chu (1975)).

The linear Darcy law which accounts for the viscous affects and is applied for slow flow in porous media was used extensively in early work on porous media. For example, the problem of natural convection in a porous medium supported by an isothermal vertical plate was solved some time ago by Cheng and Minkowycz (1977) using the Darcy law. It is well established now that the Darcy law is inapplicable for high velocity flow situations for which the relation between the pressure drop and the Darcian velocity is non-linear, and that it does not account for the presence of a boundary at which the no-slip

condition must be satisfied. Johnson and Cheng (1978), Vafai and Tien (1981) and Plumb and Huenefeld (1981) were the first to consider inertia and boundary effects in porous media.

Recently, Kou and Huang (1996a, 1996b) have developed non-similar transformations for natural convection on a vertical plate embedded in a porous medium with prescribed wall heat flux and temperature. In addition, some research has been carried out on electrically-conducting fluids such as liquid metals, water and others in the presence of magnetic field on the flow and heat transfer aspects (for example, Sparrow and Cess (1961), Gray (1979), Michiyoshi *et al.* (1976), Fumizawa (1980) and Riley (1964)). The study of heat generation or absorption effects in moving fluids is important in view of several physical problems, such as fluids undergoing exothermic or endothermic chemical reactions (see Vajravelu and Hadjinicolaou (1993) and Vajravelu and Nayfeh (1992)). In addition, Kou and Lu (1993) showed that the design of placing many electronic circuits into one small chip and more chips into package results in high volumetric heat generation in the electronic equipment. This led to the consideration of heat generation effects in porous media. In addition, recently, Chamkha (1996) analyzed the problem of non-Darcy free convection flow about a wedge and a cone embedded in a porous media in the presence of heat generation effects.

The coupled heat and mass transfer received relatively little attention. Trevisan and Bejan (1990) considered combined heat and mass transfer by natural convection in a porous medium for various geometries. Bejan and Khair (1985) reported on the natural convection boundary-layer flow in a saturated porous medium with combined heat and mass transfer. The coupled heat and mass buoyancy-induced inclined boundary layer in a porous medium was studied by Jang and Chang (1988). Later, Lai and Kulacki (1991) extended the problem of Bejan and Khair (1985) to include wall fluid injection effects. Early studies which considered coupled heat and mass transfer without the presence of porous media include the works of Gebhart and Pera (1971) on vertical plate, Pera and Gebhart (1972) and Chen and Yuh (1980) on inclined plates. Recently, Lai and Kulacki (1991) and Yih (1997) studied coupled heat and mass transfer by mixed convection from a vertical plate embedded in a fluid-saturated porous medium.

Problem formulation

Consider steady, laminar, hydromagnetic coupled heat and mass transfer by natural convection flow along a semi-infinite vertical plate embedded in a fluid-saturated porous medium as shown in Figure 1. The surface of the plate is maintained at a constant temperature or assumed to have a constant heat flux condition and a constant or variable concentration. The temperature and the concentration at the plate are always greater than their uniform ambient values existing far from the plate surface. A magnetic field of uniform strength B_o is applied in the y-direction that is normal to the plate. A constant fluid suction or blowing is imposed at the plate surface. The fluid is assumed to be Newtonian,

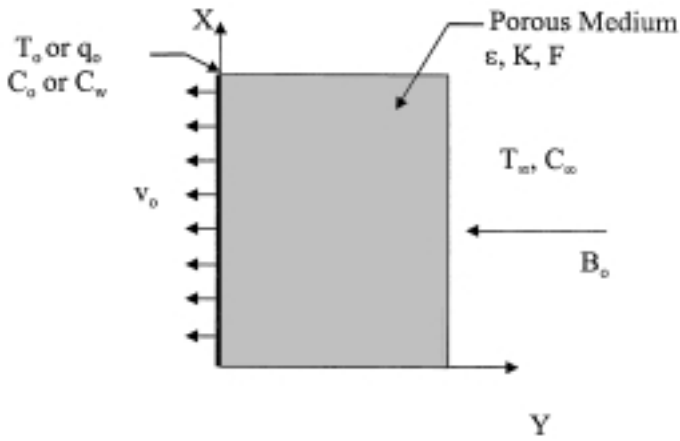

Figure 1.
Vertical plate embedded in a fluid-saturated porous medium

electrically conducting, heat generating or absorbing and has constant properties except the density in the buoyancy term of the balance of momentum equation. Also, the porosity and the permeability of the porous medium are assumed to be constant.

The magnetic Reynolds number is assumed to be small so that the induced magnetic field can be neglected. In addition, there is no applied electric field and both the Hall effect and viscous dissipation are neglected where as magnetic dissipation is considered. Invoking the Boussinesq and boundary layer approximations, the governing equations for this problem can be written as

$$\frac{\partial U}{\partial X} + \frac{\partial V}{\partial Y} = 0 \tag{1}$$

$$U\frac{\partial U}{\partial X} + V\frac{\partial U}{\partial Y} = \upsilon\frac{\partial^2 U}{\partial Y^2} + \beta_T g(T - T_\infty) + \beta_c g(C - C_\infty) - \frac{\sigma B_o^2}{\rho}U - \frac{\upsilon\varepsilon}{K}U - F\varepsilon^2 U^2 \tag{2}$$

$$U\frac{\partial T}{\partial X} + V\frac{\partial T}{\partial Y} = \alpha_e\frac{\partial^2 T}{\partial Y^2} + \frac{Q}{\rho c_p}(T - T_\infty) + \frac{\sigma B_o^2}{\rho c_p}U^2 \tag{3}$$

$$U\frac{\partial C}{\partial X} + V\frac{\partial C}{\partial Y} = D\frac{\partial^2 C}{\partial Y^2} \tag{4}$$

where U, V, T and C are the fluid x-component of velocity, y-component of velocity, temperature, and concentration, respectively. ρ, υ, c_p, β_T, and β_c are the fluid density, kinematic viscosity, specific heat at constant pressure, coefficient of thermal expansion, and coefficient of concentration expansion, respectively.

σ, Q, and D are the fluid electrical conductivity, heat generation (> 0) or absorption (< 0) coefficient, and mass diffusivity, respectively. g and B_o are the gravitational acceleration and magnetic induction, respectively. K, F, and α_e are the porous medium permeability, inertia coefficient, and effective thermal diffusivity, respectively. T_∞ and C_∞ are the ambient fluid temperature and concentration, respectively.

Non-dimensionalization of the above equations is obtained by using

$$x = \frac{X}{L}, \quad y = \frac{Y}{L}, \quad u = \frac{UL}{\alpha_e}, \quad v = \frac{VL}{\alpha_e}, \quad R = \frac{T - T_\infty}{\alpha_e \upsilon/(g\beta_T L^3)}, \quad c = \frac{C - C_\infty}{\alpha_e \upsilon/(g\beta_c L^3)} \tag{5}$$

(where L is a characteristic plate length) to give

$$\frac{\partial u}{\partial x} + \frac{\partial v}{\partial y} = 0 \tag{6}$$

$$\frac{1}{Pr}\left(u\frac{\partial u}{\partial x} + v\frac{\partial u}{\partial y}\right) + \frac{\varepsilon L^2}{K}u + \frac{F\varepsilon^2 L}{Pr}u^2 = R + c + \frac{\partial^2 u}{\partial y^2} - \frac{\sigma B_o^2 L^2}{\rho\upsilon}u \tag{7}$$

$$u\frac{\partial R}{\partial x} + v\frac{\partial R}{\partial y} = \frac{\partial^2 R}{\partial y^2} + \frac{QL^2}{k_e}R + \frac{\sigma B_o^2 g\beta_T L^3}{\rho c_p \upsilon}u^2 \tag{8}$$

$$u\frac{\partial c}{\partial x} + v\frac{\partial c}{\partial y} = \frac{1}{Le}\frac{\partial^2 c}{\partial y^2} \tag{9}$$

where $Pr = \frac{\upsilon}{\alpha_e}$ and $Le = \frac{\alpha_e}{D}$ are the Prandtl number and the Lewis number, respectively.

Isothermal wall condition

The boundary conditions in dimensional form for this case can be written as

$$\begin{array}{llll} U(X,0) = 0, & U(X,\infty) = 0, & V(X,0) = -v_o & \\ T(X,0) = T_o, & T(X,\infty) = T_\infty, & C(X,0) = C_o, & C(X,\infty) = C_\infty \end{array} \tag{10}$$

where v_o, T_o and C_o are constants representing the suction (> 0) or injection (< 0) velocity and the fluid temperature and concentration at the plate, respectively.

It is convenient herein to use the following non-similarity transformations reported earlier by Kou and Huang (1996a)

$$\eta = \frac{R_o^{1/4} y}{x^{1/4}}, \quad \xi = x, \quad f(\xi,\eta) = \frac{\psi(x,y)}{R_o^{1/4} x^{3/4}}, \quad \theta(\xi,\eta) = \frac{R(x,y)}{R_o} \tag{11}$$

Defining

$$\varsigma = \frac{c(x,y)}{c_o} \quad \text{and} \quad e = \frac{\beta_c(C_o - C_\infty)}{\beta_T(T_o - T_\infty)} \tag{12}$$

(where e is the buoyancy ratio which is the ratio of the buoyancy forces due to concentration change to the buoyancy forces due to temperature change) and substituting into equations (7)-(9) yields the following non-similar equations:

$$f''' + \frac{1}{Pr}\left[\frac{3}{4}ff'' - \frac{1}{2}(f')^2 - \xi\left(f'\frac{\partial f'}{\partial \xi} - f''\frac{\partial f}{\partial \xi}\right)\right] + \theta + e\varsigma = (A+M)\xi^{1/2} f' + \frac{B}{Pr}\xi(f')^2 \tag{13}$$

$$\theta'' + \frac{3}{4}f\theta' + \phi\xi^{1/2}\theta = \xi(f'\frac{\partial \theta}{\partial \xi} - \theta'\frac{\partial f}{\partial \xi}) - H\xi^{3/2}f'^2 \tag{14}$$

$$\frac{1}{Le}\varsigma'' + \frac{3}{4}f\varsigma' = \xi(f'\frac{\partial \varsigma}{\partial \xi} - \varsigma'\frac{\partial f}{\partial \xi}) \tag{15}$$

where a prime denotes ordinary differentiation with respect to η and

$$R_o = \frac{T_o - T_\infty}{(\upsilon\alpha_e)/(g\beta_T L^3)}, \quad c_o = \frac{C_o - C_\infty}{(\upsilon\alpha_e)/(g\beta_c L^3)}, \quad Ec = \frac{\upsilon\alpha_e}{c_p(T_o - T_\infty)L^2}$$
$$A = \frac{\varepsilon L^2}{KR_o^{1/2}}, B = F\varepsilon^2 L, \quad M = \frac{\sigma B_o^2 L^2}{\rho\upsilon R_o^{1/2}}, \phi = \frac{QL^2}{k_e R_o^{1/2}}, \quad H = Ec\,M\,R_o \tag{16}$$

are the dimensionless plate temperature, wall concentration, Eckert number, inverse Darcy number, dimensionless porous medium inertia coefficient, square of the Hartmann number, dimensionless heat generation or absorption coefficient (where k_e is the porous medium effective thermal conductivity), dimensionless magnetic dissipation coefficient, respectively. The transformed boundary conditions become

$$f'(\xi,0) = 0,\ \frac{3}{4}\xi^{-\frac{1}{4}}f(\xi,0) + \xi^{\frac{3}{4}}\frac{\partial f(\xi,0)}{\partial \xi} = V_o, \quad \theta(\xi,0) = 1,\ \varsigma(\xi,0) = 1$$
$$f'(\xi,\infty) = 0,\ \theta(\xi,\infty) = 0,\ \varsigma(\xi,\infty) = 0 \tag{17}$$

where $V_o = (v_o L)/(\alpha_e R_o^{1/4})$ is the dimensionless wall mass transfer such that $V_o > 0$ indicates suction and $V_o < 0$ indicates blowing or injection at plate surface. It should be mentioned here that when all of the parameters e, V_o, M, ϕ and H are set to zero in equations (13), (14) and (17) and ignoring equation (15), the transformed equations of Kou and Huang (1996a) are recovered.

Of special interest for this flow and heat transfer situation are the skin-friction parameter, Nusselt number, and the Sherwood number. These are defined as follows

$$\mathrm{SFP} = \frac{\tau_w}{\mu(\alpha_e/L^2)R_o^{3/4}} = \xi^{1/4} f''(\xi, 0) \tag{18}$$

$$\mathrm{Nu} = \frac{hX}{k_e} = -\xi^{3/4} R_o^{1/4} \theta'(\xi, 0) \tag{19}$$

$$\mathrm{Sh}_x = \frac{h_m X}{D} = -\xi^{3/4} R_o^{1/4} \varsigma'(\xi, 0) \tag{20}$$

where τ_w, μ, h and h_m are the shear stress at the wall, dynamic viscosity of the fluid, convective heat transfer coefficient and the local mass transfer coefficient, respectively.

Constant heat flux wall condition

For this case, the appropriate boundary conditions are

$$\begin{gathered} U(X,0) = 0, \quad U(X,\infty) = 0, \quad V(X,0) = -v_o \quad - k_e \frac{\partial T(X,0)}{\partial Y} = q_o, \\ T(X,\infty) = T_\infty, \quad C(X,0) = C_w(X), \quad C(X,\infty) = C_\infty \end{gathered} \tag{21}$$

(where q_o and $C_w(X)$ are the heat flux at the wall (a constant) and the wall concentration which is allowed to be a function of X so as to avoid singularities at X = 0, respectively).

In their work on possible transformation for natural convection over a vertical plate embedded in porous media for prescribed heat flux, Kou and Huang (1996b) suggested the following transformations:

$$\eta = \frac{Q_o^{1/5} y}{x^{1/5}}, \quad \xi = x, \quad f(\xi, \eta) = \frac{\psi(x,y)}{Q_o^{1/5} x^{4/5}}, \quad \theta(\xi, \eta) = \frac{R(x,y)}{Q_o^{4/5} x^{1/5}} \tag{22}$$

With ($\varsigma = (C - C_\infty)/(C_w - c_\infty)$), and using equations (22), the non-similar equations governing this case become

$$\begin{gathered} f''' + \frac{1}{Pr}\left[\frac{4}{5} f f'' - \frac{3}{5}(f')^2 - \xi\left(f' \frac{\partial f'}{\partial \xi} - f'' \frac{\partial f}{\partial \xi}\right)\right] + \theta + e\varsigma \\ = (A + M)\xi^{2/5} f' + \frac{B}{Pr}\xi (f')^2 \end{gathered} \tag{23}$$

$$\theta'' + \frac{4}{5} f \theta' - \frac{1}{5} f' \theta + \phi \xi^{2/5} \theta = \xi\left(f' \frac{\partial \theta}{\partial \xi} - \theta' \frac{\partial f}{\partial \xi}\right) - H\xi^{7/5} f'^2 \tag{24}$$

$$\frac{1}{Le}\varsigma'' + \frac{4}{5} f \varsigma' - \frac{1}{5} f' \varsigma = \xi\left(f' \frac{\partial \varsigma}{\partial \xi} - \varsigma' \frac{\partial f}{\partial \xi}\right) \tag{25}$$

with the concentration at the wall being in the following form

$$\frac{C_w - C_\infty}{C_{wo} - C_\infty} = \left(\frac{X}{L}\right)^{1/5} = x^{1/5} \tag{26}$$

for a constant e ($e = c_{wo}/Q_o^{4/5}$ where C_{wo} is a reference value for concentration at the wall. In equations (23)-(25),

$$Q_o = \frac{q_o}{(k_e\alpha_e\upsilon)/-(g\beta_T L^4)},\ c_{wo} = \frac{C_{wo} - C_\infty}{(\upsilon\alpha_e)/(g\beta_c L^3)},\ Ec = \frac{\upsilon\alpha_e}{c_p(q_o L^3/k_e)}$$
$$A = \frac{\varepsilon L^2}{KQ_o^{2/5}},\ B = F\varepsilon^2 L,\ M = \frac{\sigma B_o^2 L^2}{\rho\upsilon Q_o^{2/5}},\ \phi = \frac{QL^2}{k_e Q_o^{2/5}},\ H = Ec\,M\,Q_o \tag{27}$$

are the dimensionless wall heat flux, dimensionless wall concentration, Eckert number, inverse Darcy number, dimensionless porous medium inertia coefficient, square of the Hartmann number, dimensionless heat generation or absorption coefficient and the dimensionless magnetic dissipation coefficient, respectively. The transformed forms of the boundary conditions for this case become

$$f'(\xi,0) = 0,\ \frac{4}{5}\xi^{-\frac{1}{5}} f(\xi,0) + \xi^{\frac{4}{5}}\frac{\partial f(\xi,0)}{\partial\xi} = V_o,\ \theta'(\xi,0) = -1,\ \varsigma(\xi,0) = 1$$
$$f'(\xi,\infty) = 0,\ \theta(\xi,\infty) = 0,\ \varsigma(\xi,\infty) = 0 \tag{28}$$

where $V_o = (v_o L)/(\alpha_e Q_o^{1/5})$ is the dimensionless wall mass transfer for this case. Again, setting e, V_o, M, ϕ, and H to zero and ignoring equation (25) produces the transformed equations reported by Kou and Huang (1996b) for the problem of natural convection from a vertical impermeable plate maintained at uniform heat flux and embedded in a porous medium.

The skin friction parameter, Nusselt number and the Sherwood number for this case take on the following forms:

$$SFP = \frac{\tau_w}{\mu(\alpha_e/L^2)Q_o^{3/5}} = \xi^{2/5} f''(\xi,0) \tag{29}$$

$$Nu = \frac{hX}{k_e} = \xi^{4/5} Q_o^{1/5}\frac{1}{\theta(\xi,0)} \tag{30}$$

$$Sh_x = \frac{h_m X}{D} = -\xi^{4/5} Q_o^{1/5}\varsigma'(\xi,0) \tag{31}$$

The average convective heat transfer coefficient for the isothermal wall temperature condition or the constant wall heat flux condition and the average mass diffusion coefficient for both cases can be computed from the following:

$$\bar{h} = \frac{\int h dx}{\int dx}, \qquad \bar{h}_m = \frac{\int h_m dx}{\int dx} \tag{32}$$

Accordingly, Nu_{AVG} and Sh_{AVG} take on the forms

$$Nu_{AVG} = \frac{\bar{h}L}{k_e}, \qquad Sh_{AVG} = \frac{\bar{h}_m L}{D} \tag{33}$$

Numerical method

The resulting non-similar equations for both isothermal and isoflux thermal cases are non-linear and must be solved numerically with iteration subject to the corresponding boundary conditions. The implicit finite-difference method discussed by Blottner (1970) has proven to be accurate for the solution of such equations. The method starts with a change of variable such that $V = f'$ in order to reduce the momentum equations (13) and (23) into second-order non-similar equations. Then, the equations governing V, θ, and ς for both isothermal and isoflux cases will have the general form

$$\pi_1 Z'' + \pi_2 Z' + \pi_3 Z + \pi_4 = 0 \tag{34}$$

where Z is a typical dependent variable and the πs are functions of the dependent and independent variables.

At the i^{th} stage of the iteration process, linear equations are created by evaluating the dependent variables appearing in the πs in equation (34) using the last value produced by the iteration process. These equations are then discretized using three-point variable-step difference quotients to give a set of linear algebraic equations for each of the dependent variables of the form

$$A_n(Z_i)_{n-1} + B_n(Z_i)_n + C_n(Z_i)_{n+1} = D_n \tag{35}$$

where A_n, B_n, C_n and D_n are functions of the πs and the step sizes used in the η direction. The subscripts i and n denote the i^{th} iteration and the n^{th} point along the η direction, respectively.

The non-similar equations become similar at $\xi = 0$. Hence, the πs will only be functions of the dependent variables. For $\xi \neq 0$, the first derivatives in ξ are discretized by using two point backward difference formulas so that the πs will be functions of the independent variables and dependent variables at the current and previous lines of ξ.

Equation (35) represents a tri-diagonal set of N-2 linear algebraic equations that are solved by the well-known Thomas algorithm. A variable step in the η direction is selected since rapid changes in the dependent variables are expected near the wall. With a starting step size in the η direction of 0.001 at the wall and a step size growth factor of 1.03 such that $\Delta\eta_{n+1} = 1.03\Delta\eta_n$, accurate results can be obtained with minimum computational efforts. Moreover, a constant step of 0.005 in the ξ direction was selected after performing many

trials to assess grid independence. The convergence criterion for this problem required that the difference between the current and the previous iterations be 10^{-8}. Once the solutions for V, θ and ς are converged, the equation $V = f'$ is solved for $f(\eta)$ by the trapezoidal rule. This solution procedure is done for the non-similar equations obtained for both constant temperature and constant heat flux wall conditions. A representative set of graphical results is presented in Figures 2-11 to show the influence of the physical parameters on the solutions. It should be noted that in the reference parametric conditions employed to obtain the graphical results, e, H, and ϕ were set to zero. This is done intentionally to reduce the number of figures as by doing this, the concentration profiles will be the same as the temperature profiles.

It should be mentioned here that the above numerical method was employed to solve the non-similar equations excluding all of the magnetic, heat generation or absorption, and the porous media terms and ignoring the mass diffusion equation. The results of f′, θ and Nu were found to be in excellent agreement with the solution of laminar natural convection boundary layer flow along a vertical wall with both constant wall temperature and constant wall heat flux reported by Bejan (1993) and Sparrow (1955), respectively. These comparisons lend confidence in the adequacy and accuracy of the numerical method.

Useful correlations

1st – constant wall temperature condition

In this section some correlations for both Nu_{AVG} and Sh_{AVG} for various combinations of the physical parameters are reported.

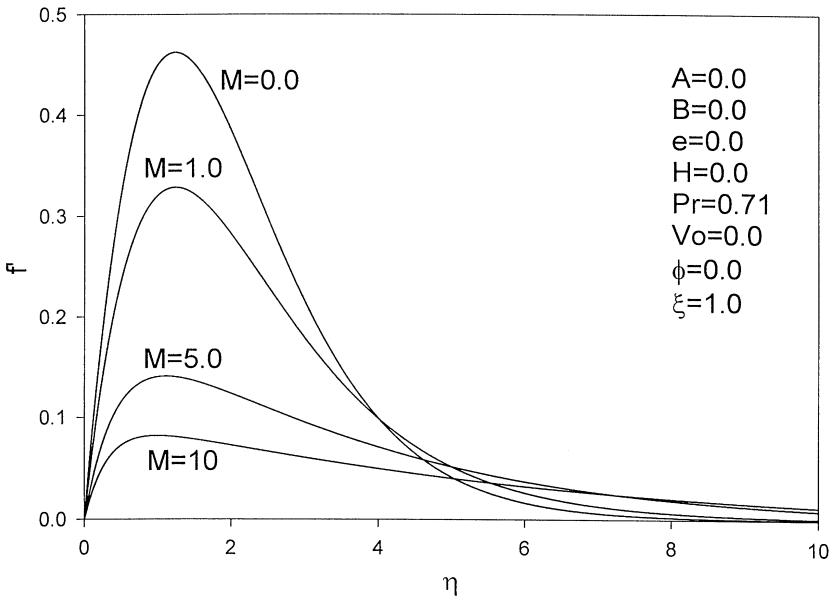

Figure 2.
Effects of M on tangential velocity profile for (UWT)

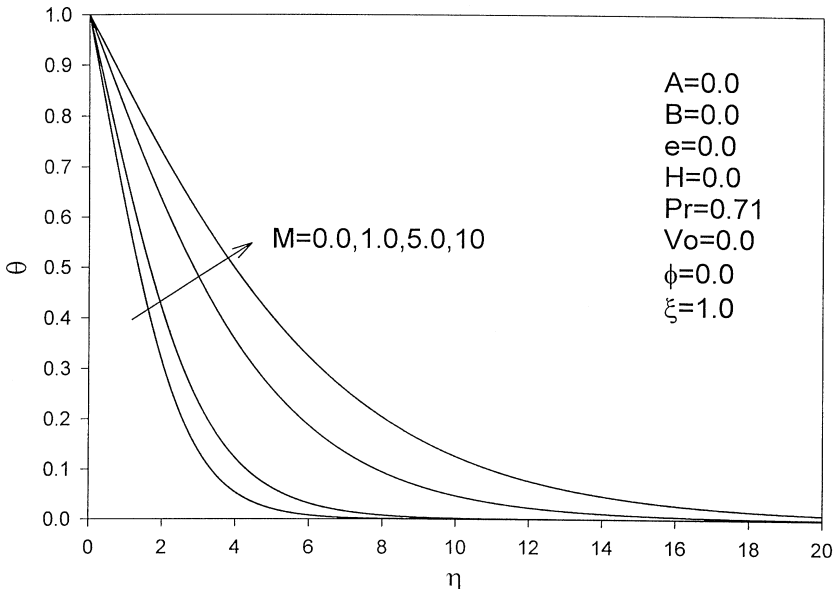

Figure 3.
Effects of M on temperature profiles for (UWT)

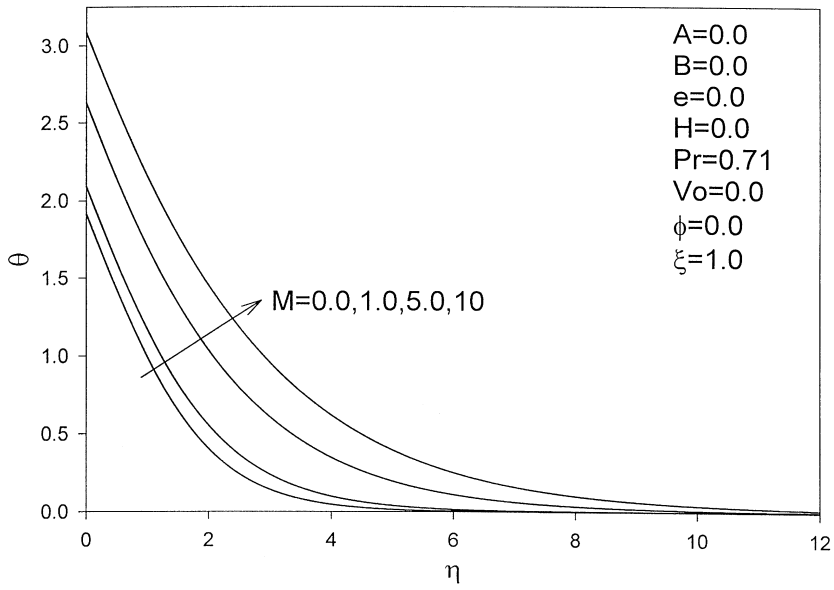

Figure 4.
Effects of M on temperature profiles for (UHF)

(a) The following correlations for Nu_{AVG} and Sh_{AVG} as functions of Pr and R_o are suitable for Le = 0.5, 0.71 < Pr < 10 and all of A, B, e, M, V_o and ϕ are set to zero with maximum errors less than 1 per cent and 1.5 per cent, respectively.

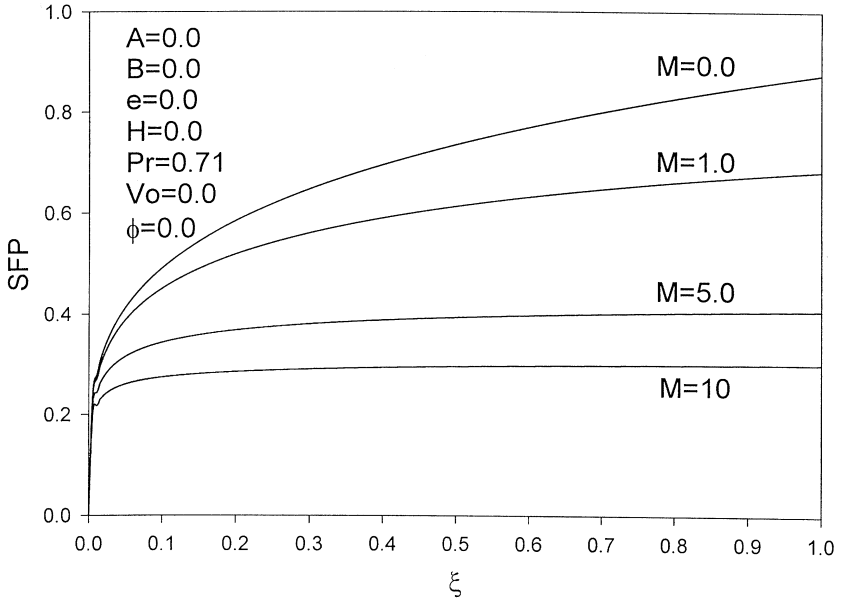

Figure 5.
Effects of M on the local skin friction parameter for (UWT)

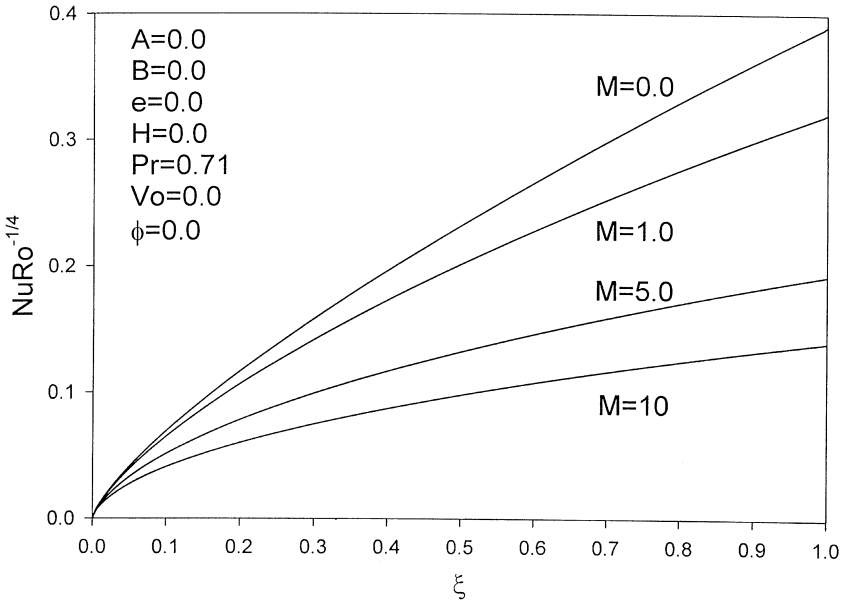

Figure 6.
Effects of M on the local Nusselt number for (UWT)

$$\mathrm{Nu_{AVG}} = 0.5278\,\mathrm{R_o^{1/4}}\ \mathrm{Pr}^{0.06921} \tag{C1}$$

$$\mathrm{Sh_{AVG}} = 0.3679\,\mathrm{R_o^{1/4}}\ \mathrm{Pr}^{0.0983} \tag{C2}$$

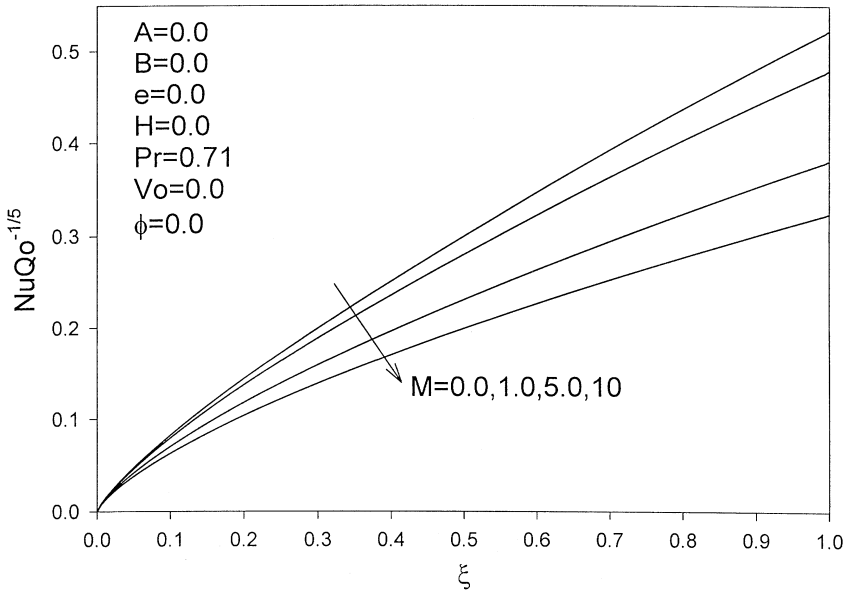

Figure 7.
Effects of M on the local Nusselt number for (UHF)

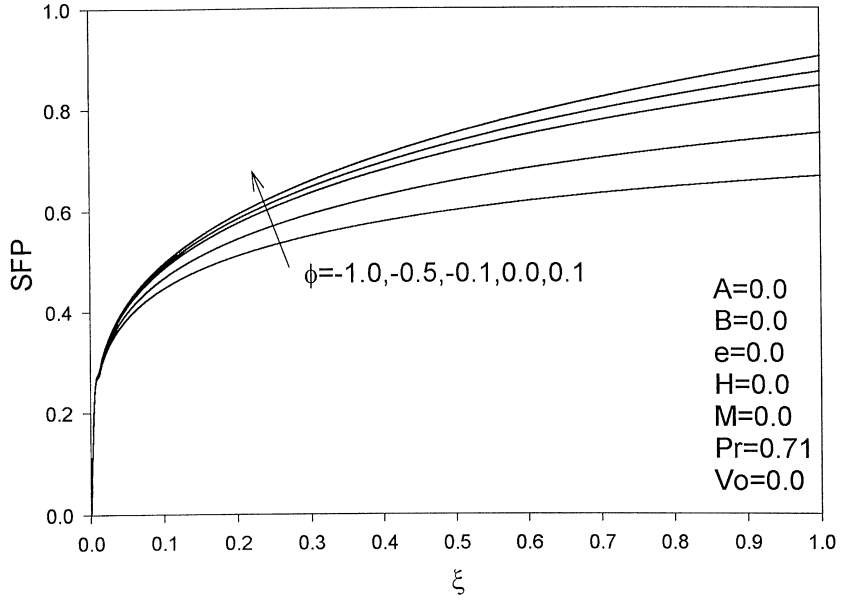

Figure 8.
Effects of ϕ on the local skin friction parameter for (UWT)

(b) The following correlations for Nu_{AVG} and Sh_{AVG} as functions of M or A and R_o are suitable for Le = 0.5, Pr = 0.71, and all of B, e, V_o and ϕ are set to zero, 0 < A, M < 10 with maximum errors less than 4 per cent and 5 per cent, respectively.

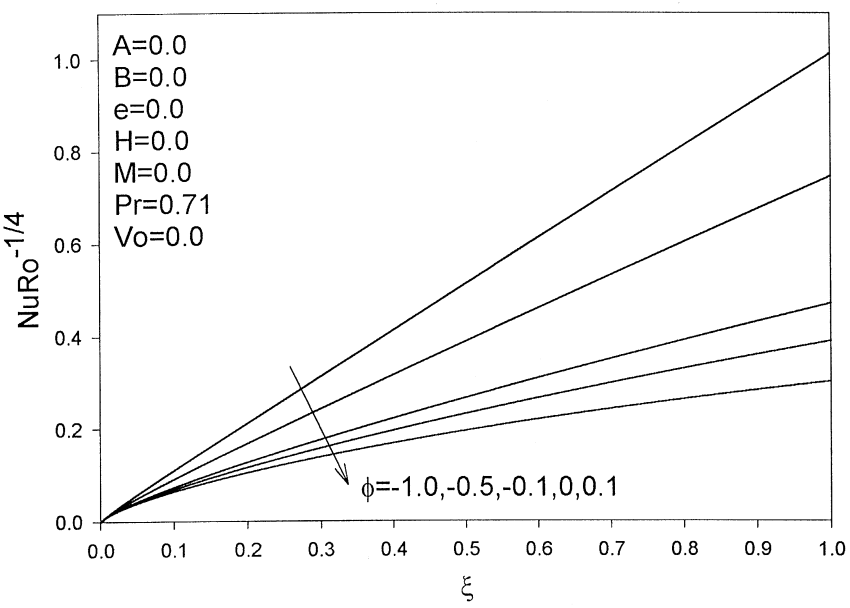

Figure 9.
Effects of ϕ on the local Nusselt number for (UWT)

$$\mathrm{Nu_{AVG}} = \frac{0.5270}{(1 + \mathrm{M, A})^{0.2849}}\ \mathrm{R_o^{1/4}} \tag{C3}$$

$$\mathrm{Sh_{AVG}} = \frac{0.3603}{(1 + \mathrm{M, A})^{0.3160}}\ \mathrm{R_o^{1/4}} \tag{C4}$$

(c) The following correlations for $\mathrm{Nu_{AVG}}$ and $\mathrm{Sh_{AVG}}$ as functions of $\mathrm{V_o}$ and $\mathrm{R_o}$ are suitable for Le = 0.5, Pr = 0.71, $-0.1 < \mathrm{V_o} < 0.5$ and all of A, B, e, M and ϕ are set to zero with maximum errors less than 3.5 per cent and 3 per cent, respectively.

$$\mathrm{Nu_{AVG}} = 0.8323\,|\mathrm{V_o} + 0.3754|^{\,0.4803}\mathrm{R_o^{1/4}} \tag{C5}$$

$$\mathrm{Sh_{AVG}} = 0.4847\,|\mathrm{V_o} + 0.3723|^{0.3165}\ \mathrm{R_o^{1/4}} \tag{C6}$$

Note that linear correlations can be associated to the range $-0.5 < \mathrm{V_o} < -0.1$ with the limit values evaluated from correlations (5) and (6).

(d) The following correlations for $\mathrm{Nu_{AVG}}$ and $\mathrm{Sh_{AVG}}$ as functions of ϕ and $\mathrm{R_o}$ are suitable for Le = 0.5, Pr = 0.71, $-1.0 < \phi < 0.1$ and all of A, B, e, M and $\mathrm{V_o}$ are set to zero with maximum errors less than 0.5 per cent for both correlations.

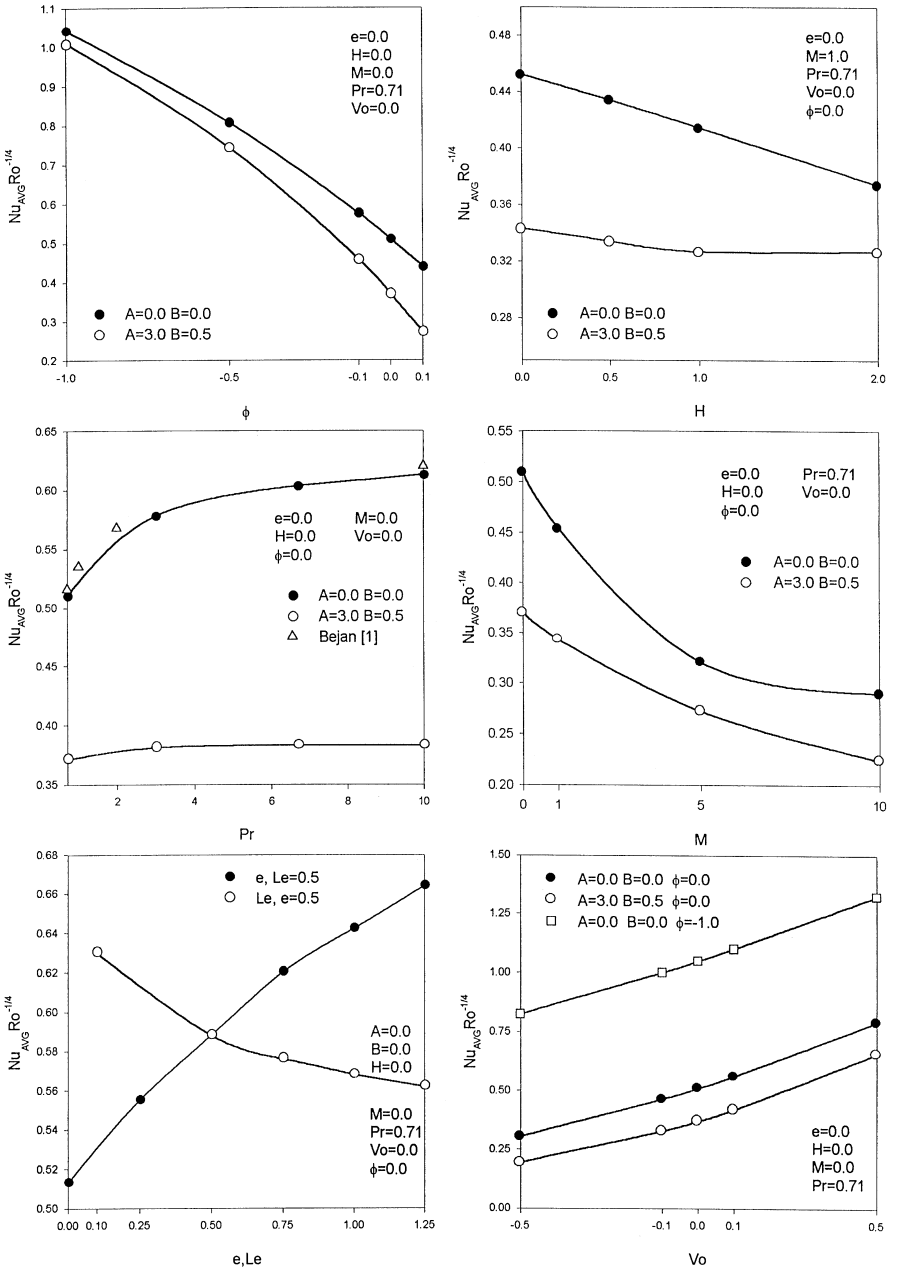

Figure 10.
Effects of A, B, e, H, Le, M, Pr, V_o and ϕ on average Nusselt number for (UWT)

$$Nu_{AVG} = 0.8270\,|\phi - 0.460|^{0.6175}\,R_o^{1/4} \qquad (C7)$$

$$Sh_{AVG} = 0.3579\,|\phi + 0.8412|^{0.1093}\,R_o^{1/4} \qquad (C8)$$

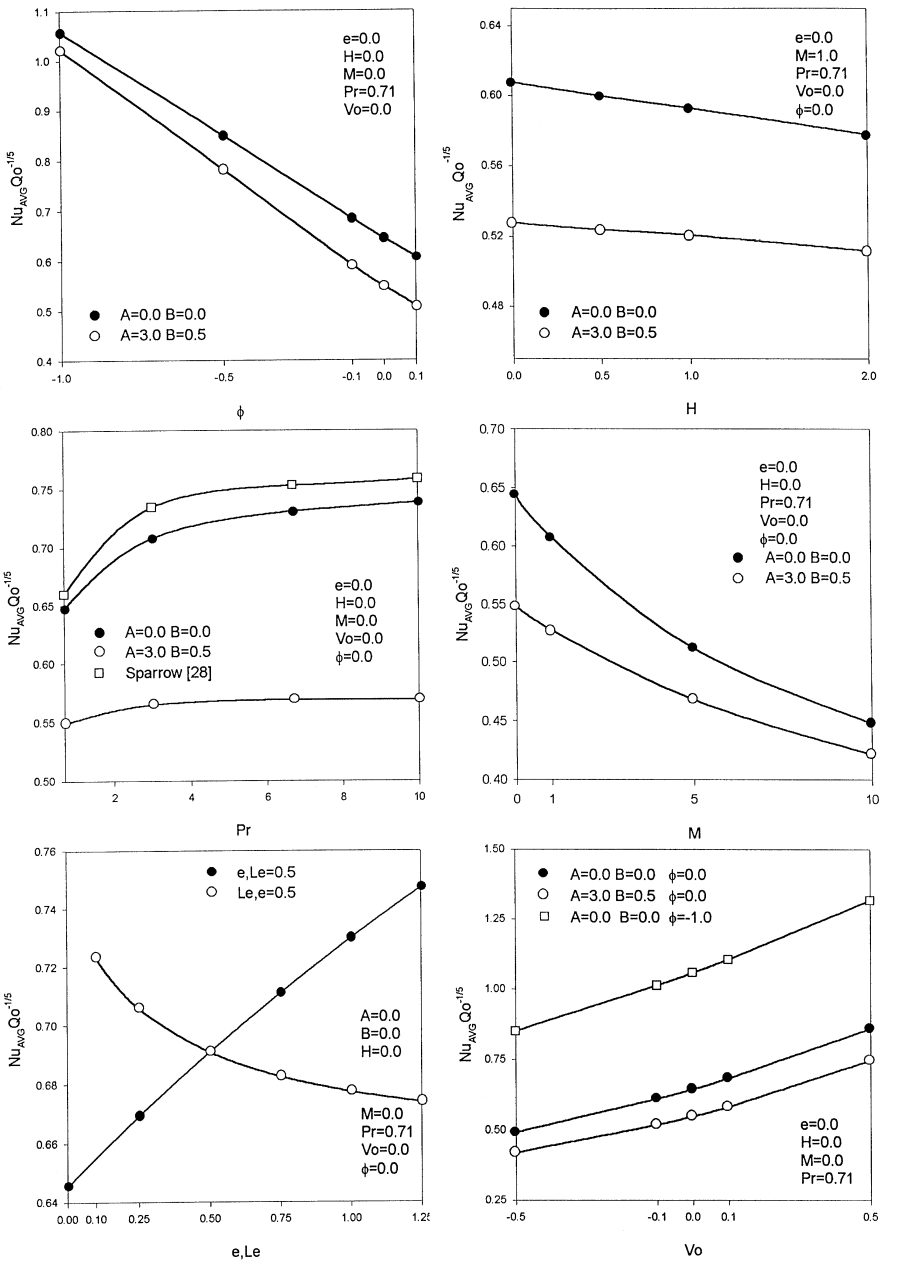

Figure 11.
Effects of A, B, e, H, Le, M, Pr, V_o and ϕ on average Nusselt number for (UHF)

(e) The following correlations for Nu_{AVG} and Sh_{AVG} as functions of e, Le and R_o are suitable for $Pr = 0.71$, $0 < e < 2$, $0.1 < Le < 100$ and all of A, B, M, V_o and ϕ are set to zero with maximum error less than 15 per cent and 11 per cent, respectively.

$$\mathrm{Nu_{AVG}} = \left(0.5698 + 0.0907\mathrm{e} - 0.01158\mathrm{Le} - 0.01559\mathrm{e}^2 + 0.000105\mathrm{Le}^2\right)\mathrm{R_o^{1/4}} \quad \text{(C9)}$$

$$\mathrm{Sh_{AVG}} = \left(0.4355 + 0.1371\mathrm{e} + 0.1059\mathrm{Le} - 0.0143\mathrm{e}^2 - 0.0008\mathrm{Le}^2\right)\mathrm{R_o^{1/4}} \quad \text{(C10)}$$

(f) The following correlations for $\mathrm{Nu_{AVG}}$ and $\mathrm{Sh_{AVG}}$ as functions of Pr, A and $\mathrm{R_o}$ are suitable for $1 < \mathrm{A} < 10$, $0.71 < \mathrm{Pr} < 10$ with e = 0.0, Le = 0.5 and all of B, M, $\mathrm{V_o}$ and ϕ are set to zero with maximum errors less than 5 per cent and 7 per cent, respectively.

$$\frac{\mathrm{Nu_{AVG}(A, Pr)}}{\mathrm{Nu_{AVG}(A = 0.0, Pr)}} = \frac{0.8455\mathrm{Pr}^{0.0009}}{\mathrm{A}^{0.3155}} \quad \text{(C11)}$$

$$\frac{\mathrm{Sh_{AVG}(A, Pr)}}{\mathrm{Sh_{AVG}(A = 0.0, Pr)}} = \frac{0.8065\mathrm{Pr}^{0.0001}}{\mathrm{A}^{0.3667}} \quad \text{(C12)}$$

2nd – constant wall heat flux condition

For the subsequent correlations which result from the solution of combined heat and mass transfer by natural convection over a semi-infinite vertical plate maintained at constant heat flux condition, all of the parameters A, B, e, H, Le, M, Pr, $\mathrm{V_o}$ and ϕ are assumed zero unless otherwise stated.

(a) The following correlations for $\mathrm{Nu_{AVG}}$ and $\mathrm{Sh_{AVG}}$ as functions of Pr and $\mathrm{Q_o}$ are suitable for $0.71 < \mathrm{Pr} < 10$ and Le = 0.5 with maximum errors less than 1 per cent and 2 per cent, respectively.

$$\mathrm{Nu_{AVG}} = 0.6611\mathrm{Q_o^{1/5}Pr}^{0.0516} \quad \text{(C13)}$$

$$\mathrm{Sh_{AVG}} = 0.4638\mathrm{Q_o^{1/5}Pr}^{0.0782} \quad \text{(C14)}$$

(b) The following correlations for $\mathrm{Nu_{AVG}}$ and $\mathrm{Sh_{AVG}}$ as functions of M or A for the range $0 < \mathrm{M}, \mathrm{A} < 10$ and $\mathrm{Q_o}$ are suitable for Pr = 0.71 with the remaining A or M set to zero and Le = 0.5 with maximum errors less than 3 per cent and 3.5 per cent, respectively.

$$\mathrm{Nu_{AVG}} = \frac{0.6568}{(1 + \mathrm{M, A})^{0.1484}}\mathrm{Q_o^{1/5}} \quad \text{(C15)}$$

$$\mathrm{Sh_{AVG}} = \frac{0.4556}{(1 + \mathrm{M, A})^{0.2014}}\mathrm{Q_o^{1/5}} \quad \text{(C16)}$$

(c) The following correlations for Nu_{AVG} and Sh_{AVG} as functions of the dimensionless wall mass transfer V_o in the range $-0.1 < V_o < 0.5$ and Q_o are suitable for Pr = 0.71 and Le = 0.5 with maximum errors less than 3 per cent and 1.5 per cent, respectively.

$$Nu_{AVG} = 0.8834|V_o + 0.3604|^{0.2955} Q_o^{1/5} \tag{C17}$$

$$Sh_{AVG} = 0.5410|V_o + 0.3642|^{0.1817} Q_o^{1/5} \tag{C18}$$

Note that linear correlations can be associated to Nu_{AVG} and Sh_{AVG} with limit values evaluated from correlations (17) and (18) for the range $-0.5 < V_o < -0.1$.

(d) The following correlations for Nu_{AVG} and Sh_{AVG} as functions of Q_o and ϕ, for the range $-1.0 < \phi < 0.1$ for calculating Nu_{AVG} and for the range $-0.7 < \phi < 0.1$ for calculating Sh_{AVG}, are suitable for Pr = 0.71 and Le = 0.5 with maximum errors less than 0.2 per cent and 1 per cent, respectively.

$$Nu_{AVG} = 0.3174|\phi + 1.8590|^{0.1464} Q_o^{1/5} \tag{C19}$$

$$Sh_{AVG} = 0.4596|\phi + 0.8475|^{0.1615} Q_o^{1/5} \tag{C20}$$

(e) The following correlations for Nu_{AVG} and Sh_{AVG} as functions of e, Le and Q_o are suitable for Pr = 0.71, $0 < e < 10$ and $0.1 < Le < 100$ but for the calculation of the Sh_{AVG} the range of Le is $1 < Le < 100$ with maximum errors less than 18 per cent and 8 per cent, respectively. The large percentages of correlation deviations from the numerical solution were found to appear for large values of the buoyancy ratio e especially as $e \to 10$.

$$Nu_{AVG} = (0.7239 + 0.0518e - 0.0144Le - 0.00246e^2 + 0.000129Le^2) Q_o^{1/5} \tag{C21}$$

$$Sh_{AVG} = (0.4670 + 0.07828e + 0.1324Le - 0.002445e^2 + 0.0009771Le^2) Q_o^{1/5} \tag{C22}$$

(f) The following correlations for Nu_{AVG} and Sh_{AVG} as functions of A, Pr and Q_o are suitable for e = 0.0, $1 < A < 10$ and $0.71 < Pr < 10$ with maximum errors about 3 per cent and 7 per cent for Nu_{AVG} and Sh_{AVG}, respectively.

$$\frac{\mathrm{Nu_{AVG}(A,Pr)}}{\mathrm{Nu_{AVG}(A=0.0,Pr)}} = \frac{0.9113\mathrm{Pr}^{0.005}}{\mathrm{A}^{0.1716}} \quad \text{(C23)}$$

$$\frac{\mathrm{Sh_{AVG}(A,Pr)}}{\mathrm{Sh_{AVG}(A=0.0,Pr)}} = \frac{0.8634\mathrm{Pr}^{0.0054}}{\mathrm{A}^{0.2381}} \quad \text{(C24)}$$

Results and discussion

Figures 2 and 3 present representative velocity and temperature profiles at $\xi = 1$ for various values of the square of the Hartmann number M for the case of isothermal wall, respectively. It is a known fact that application of a transverse magnetic field normal to the flow direction results in a flow-resistive force called the Lorentz force which acts in the opposite direction of flow. This force has the effect of slowing the motion of the fluid and increasing its temperature and concentration with increases in all of the hydrodynamic, thermal, and concentration boundary layer thicknesses. It should be noted that, for the isothermal case, the concentration profiles are similar to the temperature profiles when Le = 1 and ϕ = H = 0 since they are governed by similar differential equations and boundary conditions. The thermal condition of constant wall heat flux results in a similar trend as in the isothermal wall case except that the wall temperature increases as the square of the Hartmann number increases as shown by Figure 4.

Figures 5 and 6 illustrate the influence of the magnetic parameter (square of the Hartmann number) M on the development of the local skin-friction parameter SFP and the local Nusselt number $\mathrm{Nu^T}$ (= $\mathrm{NuR_o^{-1/4}}$) along the isothermal plate, respectively. On the other hand, Figure 7 presents the local Nusselt number $\mathrm{Nu^Q}$ (= $\mathrm{NuQ_o^{-1/5}}$) for the isoflux wall condition. As a result of the slowing motion of the fluid caused by the presence of the Lorentz force, the wall slope of the velocity profile decreases. This has the direct effect of reducing the wall shear stress represented by SFP. However, the wall slope of the temperature profile for the isothermal plate case decreases and the wall temperature for the constant heat flux case increases as M increases. This produces lower Nusselt number values for both cases at every point along the plate. These behaviors are depicted by the decreases in the values of SFP, $\mathrm{Nu^T}$ and $\mathrm{Nu^Q}$ as M increases, displayed in Figures 5, 6 and 7, respectively. It is worth mentioning that the definition of the magnetic parameter M for both cases is different. Thus, different responses in $\mathrm{Nu^T}$ and $\mathrm{Nu^Q}$ can be noticed as M is altered. It is also observed that all of SFP, $\mathrm{Nu^T}$, and $\mathrm{Nu^Q}$ have an increasing behavior with the tangential distance ξ. It should be mentioned that similar to the Nusselt number, the Sherwood number decreases as M increases.

Similar to the magnetic field effect on electrically-conducting fluids, the effect of the presence of the porous medium is to slow the motion of the fluid and to increase its temperature and concentration. This flow resistance mechanism increases as either of the inverse Darcy number A, the dimensionless porous

medium inertia coefficient B, or both increase. As mentioned before, this causes the values of SFP, Nu^T and Sh^T ($= Sh_x R_o^{-1/4}$) to decrease. In a similar manner, the case of constant wall heat flux produces similar trends taking into account that the Darcy number is different for both cases and the inertia coefficients are the same. These results are not presented herein for brevity.

In general, imposition of fluid suction at the wall has a tendency to decrease the thermal boundary layer for both studied cases. This causes the fluid temperature profile and its slope at the wall for the (UWT) case to increase or the wall temperature for the uniform wall heat flux (UHF) case to decrease. This results in enhancement of the wall heat transfer represented by increases in the Nusselt number. In addition, the values of the skin-friction parameter SFP increase as the suction parameter increases. The same can be said for the uniform wall heat flux.

In Figures 8 and 9, the effects of heat absorption or generation for constant wall temperature on the skin-friction parameter and the Nusselt number are shown. It is observed that higher values of ϕ causes higher fluid temperatures and, therefore, higher thermal buoyancy effects. This produces higher velocity flow along the plate. These behaviors result in higher wall velocity and temperature slopes which produce higher SFP and lower Nu^T values, respectively. These facts are clear from Figures 8 and 9. Similarly, the Nusselt number for the uniform heat flux case exhibits similar features as the internal heat generation or absorption parameter changes.

As expected, the increases in the values of the buoyancy ratio e cause increases in the total buoyancy effect and, therefore, increases in the flow induced by this effect. This is done at the expense of both the fluid temperature and concentration. As a result of this and as explained before, the values of SFP, Nu^T and Sh^T tend to increase as e increases.

In Figure 10, a parametric study illustrating the effects of the Darcy number A, inertia coefficient B, buoyancy ratio e, magnetic dissipation parameter H, Prandtl number Pr, wall mass transfer parameter V_o and the internal heat generation or absorption parameter ϕ on the average Nusselt number for the case of constant wall temperature is conducted. With fluids of high Prandtl number, the thermal boundary layer becomes thinner and as a result an increase in Nu_{AVG} is expected. A good agreement with the results reported by Bejan (1993) on the buoyancy-induced flow over a vertical impermeable plate is observed in the third figure from top of Figure 10. From previous discussion and knowing that Nu_{AVG} is the integral of the local Nusselt number over the plate length, the Nu_{AVG} decreases as either of ϕ, A, B or M increases and increases as V_o or e increases. The presence of the magnetic dissipation parameter H decreases Nu_{AVG} since the term containing H acts as an internal heat generation mechanism. Recalling that the Lewis number is different for variable combination of fluid and diffused species. If the species have a higher tendency to diffuse into the fluid, the Lewis number will be lower. Thus, as Le decreases, Nu_{AVG} increases. Similar qualitative trends are shown in Figure 11 for the case of uniform wall heat flux. In this case, the numerical results for

Nu_{AVG} are validated with the integral solution of Sparrow (1955) for the problem of natural convection over a vertical plate with constant wall heat flux excluding the terms containing A, B, e, M, V_o and ϕ. The apparent discrepancy between the present results and those of Sparrow (1955) is due to the fact that Sparrow (1955) uses a less accurate approximate integral method than the more accurate implicit finite-difference numerical method of the present work.

Conclusion

The problem of steady, laminar, hydromagnetic heat and mass buoyancy-induced natural convection boundary-layer flow of an electrically-conducting and heat generating or absorbing fluid along an isothermal or isoflux vertical and permeable semi-infinite surface embedded in a uniform porous medium was considered. The governing equations for both situations of uniform wall temperature (UWT) and uniform wall heat flux (UHF) were developed and transformed using appropriate non-similarity transformations. The transformed equations were then solved numerically by an implicit, iterative, finite-difference scheme. The obtained results for special cases of the problem were compared with previously published work and found to be in excellent agreement. Useful correlations for both isothermal and isoflux wall conditions were reported for various physical parameters. It was found that while all of the skin-friction parameter, Nusselt number and the Sherwood number decreased as a result of the presence of either the magnetic field or the porous medium, they increased due to imposition of fluid suction at the plate surface for both the uniform wall temperature and the uniform wall heat flux cases. Also, the skin-friction parameter was increased and the Nusselt number were decreased due to the presence of heat generation effects for both cases. Furthermore, increasing the ratio of concentration to thermal buoyancies was found to cause enhancements in the values of the skin-friction parameter, Nusselt number and the Sherwood number for the two studied thermal cases. It is hoped that the present work will serve as a vehicle for understanding more complex problems involving the various physical effects investigated in the present problem.

References

Bejan, A. (1993), *Convection Heat Transfer*, 2nd ed., Wiley, New York, NY, p. 176.

Bejan, A. and Khair, K.R. (1985), "Heat and mass transfer by natural convection in a porous medium", *Int. Commun. Heat Mass Transfer*, Vol. 28, pp. 909-18.

Blottner, F.G. (1970), Finite-difference methods of solution of the boundary-layer equations", *AIAA Journal*, Vol. 8, pp. 193-205.

Chamkha, A.J. (1996), "Non-Darcy hydromagnetic free convection from a cone and a wedge in porous media", *Int. Commun. Heat Mass Transfer*, Vol. 23, pp. 875-87.

Cheng, P. and Minkowycz, W.J. (1977), "Free convection about a vertical flat plate embedded in a porous medium with application to heat transfer from a dike", *J. of Geophy. Res.*, Vol. 82, pp. 2040-4.

Chen, T.S. and Yuh, C.F. (1980), "Combined heat and mass transfer in mixed convection along vertical and inclined plates", *Int. J. Heat Mass Transfer*, Vol. 23, pp. 527-37.

Churchill, S.W. and Chu, H.H.S. (1975), "Correlating equations for laminar and turbulent free convection from a vertical plate", *Int. J. Heat Mass Transfer*, Vol. 18, pp. 1323-9.

Fumizawa, M. (1980), "Natural convection experiment with liquid NaK under transverse magnetic field", *J. Nuclear Science and Technology*, Vol. 17, pp. 10-17.

Gebhart, B. and Pera, L. (1971), "The nature of vertical natural convection flows resulting from the combined buoyancy effects of thermal and mass diffusion", *Int. J. Heat Mass Transfer*, Vol. 14, pp. 2025-50.

Gray, D.D. (1979), "The laminar wall plume in a transverse magnetic field", *Int. Commun. Heat Mass Transfer*, Vol. 22, pp. 1155-8.

Jang, J.Y. and Chang, W.J. (1988), "Buoyancy-induced inclined boundary layer flow in a porous medium resulting from combined heat and mass buoyancy effects", *Int. Commun. Heat Mass Transfer*, Vol. 15, pp. 17-30.

Johnson, C.H. and Cheng, P. (1978), "Possible similarity solutions for free convection boundary-layers adjacent to flat plates in porous media", *Int. J. Heat Mass Transfer*, Vol. 21, pp. 709-18.

Kou, H. and Huang, D. (1996a), "Some transformations for natural convection on a vertical plate embedded in porous media with prescribed wall temperatures", *Int. Commun. Heat Mass Transfer*, Vol. 23, pp. 273-86.

Kou, H. and Huang, D. (1996b), "Possible transformations for natural convection on a vertical plate embedded in porous media with prescribed wall heat flux", *Int. Commun. Heat Mass Transfer*, Vol. 23, pp. 1031-42.

Kou, H.S. and Lu, K.T. (1993), "Combined boundary and inertia effects for fully developed mixed convection in a vertical channel embedded in porous media", *Int. Commun. Heat Mass Transfer*, Vol. 20, pp. 333-45.

Lai, F.C. and Kulacki, F.A. (1991), "Non-Darcy mixed convection along a vertical wall in a saturated porous medium", *Int. J. Heat Mass Transfer*, Vol. 113, pp. 252-5.

Michiyoshi, I., Takahashi, I. and Serizawa, A. (1976), "Natural convection heat transfer from a horizontal cylinder to mercury under magnetic field", *Int. J. Heat Mass Transfer*, Vol. 19, pp. 1021-9.

Pera, L. and Gebhart, B. (1972), "Natural convection boundary layer flow over horizontal and slightly inclined surfaces", *Int. J. Heat Mass Transfer*, Vol. 16, pp. 1131-46.

Plumb, O.A. and Huenefeld, T.C. (1981), "Non-Darcy natural-convection from heated surfaces in saturated porous media", *Int. J. Heat Mass Transfer*, Vol. 24, pp. 765-8.

Riley, N. (1964), "Magnetohydrodynamics free convection", *J. Fluid Mech.*, Vol. 18, pp. 577-86.

Sparrow, E.M. (1955), "Laminar free convection from a vertical plate with prescribed nonuniform wall heat flux or prescribed nonuniform wall temperature", *NACA TN 3508*, July.

Sparrow, E.M. and Cess, R.D. (1961), "Effects of magnetic field on free convection heat transfer", *Int. J. Heat Mass Transfer*, Vol. 3, pp. 267-74.

Trevisan, O.V. and Bejan, A. (1990), "Mass and heat transfer by natural convection in a vertical slot filled with porous medium", *Int. J. Heat Mass Transfer*, Vol. 29, pp. 403-15.

Vafai, K. and Tien, C.L. (1981), "Boundary and inertia effects on flow and heat transfer in porous media", *Int. J. Heat Mass Transfer*, Vol. 24, pp. 195-203.

Vajravelu, K. and Hadjinicolaou, A. (1993), "Heat transfer in a viscous fluid over a stretching sheet with viscous dissipation and internal heat generation", *Int. Commun. Heat Mass Transfer*, Vol. 20, pp. 417-30.

Vajravelu, K. and Nayfeh, J. (1992), "Hydromagnetic convection at a cone and a wedge", *Int. Commun. Heat Mass Transfer*, Vol. 19, pp. 701-10.

Yih, K.A. (1997), "The effect of transpiration on coupled heat and mass transfer in mixed convection over a vertical plate embedded in a saturated porous medium", *Int. Commun. Heat Mass Transfer*, Vol. 24, pp. 265-75.